24th COBEM - 2017

24th ABCM International Congress of Mechanical Engineering
December 3-8, 2017, Curitiba, PR, Brazil

COBEM-2017-2455
SLIDING MODE CONTROL OF A FLEXIBLE ROTATING SYSTEM SUBJECT TO CONCENTRATED DRY FRICTION

Adriano Domeny dos Santos
Agenor de Toledo Fleury
Escola Politécnica da Universidade de São Paulo, Department of Mechanical Engineering, São Paulo, Brazil
adrianodomeny@usp.br, agenorfleury@usp.br

Abstract. *The aim of this work is to present the results of the implementation of a robust control technique - sliding control - to stabilize the angular velocity of a slim and flexible rotary system, subject to dry friction. The system is considered full observable. As a result of the simulations, a phase diagram with the usual state variables is achieved indicating the system trajectory from rest to reaching a desired state. This study contributes to a better understanding of a real problem involving drilling systems for oil and gas wells.*

Keywords: *sliding mode, rotary system, dry friction, torsional dynamics and eigenfunctions.*

1. INTRODUCTION

In oil well drilling systems, an extremely slim cylindrical column is used to transfer rotational energy to a drill bit near oil and gas extraction field. A column like that can reach 5km length. Both, column and drill are subject to a friction regime in the interaction with the walls of the hole, which leads to the generation of undesired phenomena. From the other side, drilling rate is the main parameter to characterize process efficiency. Understanding the reasons for an eventual instability is, than, mandatory.

There are some works in the literature with sliding modes applications to stabilize rotary drilling systems. López and Castro (2009) use a dynamical model based in concentrated parameters, and a function that defines the induced sliding regime for the system. Abdulgalil and Siguedidjane (2005) utilize a concentrated parameter model for rotary system subject to stick-slip oscillations where the controller is a PID based on sliding mode control. López and Cortés (2007) use sliding mode to accomplish the control goal of driving the rotary velocities system to prespecified values despite variations in the weight on the bit. Zhang, *et al.*, 2010 implement a robust hybrid controller based on feedback linearization, sliding mode and PID controller.

Inspired by the real drilling system, the aim of this work is to present the results of the implementation of a robust control technique - sliding control - to stabilize the angular velocity of a slim and flexible rotary system, subject to dry friction.

2. MATHEMATIC MODEL

2.1 Dynamic model

The test bench is built as illustrated in Fig. 1. It is composed by a DC motor and a metallic rotor coupled by a slender and flexible metallic axis. Recent work (Andrade, 2011) shows a similar test bench.

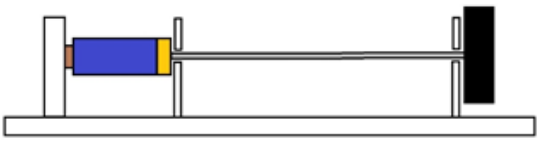

Figure 1. The test bench. A DC motor and a metallic rotor coupled by a slender and flexible metallic axis.

System is physically a double rotor model, since it considers the internal rotor of the motor and the external rotor, coupled by the slender axis. Chosen input of the plant is the input voltage in the motor; and the output variable to be

controlled is the angular velocity of the external rotor. A dry friction torque is applied on the external rotor, as a function of the angular velocity, according to Eq. (1). Christoforou (2005) use a similar model.

$$F\left(\theta,\dot{\theta}\right)=\mu\left(\dot{\theta}\right)N(\theta)R_s \tag{1}$$

θ is the angular position of the external rotor, and R_s is the distance between external rotor center and point of friction application on the external rotor.

The function $\mu\left(\dot{\theta}\right)=\mu_0\Phi(\upsilon),\ \upsilon=\dfrac{\dot{\theta}}{\omega_0}$, is the dry friction coefficient as a function of angular velocity $\dot{\theta}$, and ω_0 is nominal angular velocity.

$\Phi(\upsilon)=\tanh(\upsilon)+\dfrac{\alpha_1\upsilon}{1+\alpha_2\upsilon^2}$ is a dimensionless function with parameters α_1 and α_2.

$N(\theta)=N_0\left(1+\beta_N \operatorname{sen}(\theta)\right)$ is the normal force as a function of angular position.

Table 1 shows some data about the test bench.

Table 1. Bench data.

Properties	Measurements
Axis length (mm)	2500
Axis diameter (mm)	6.0
Rotor diameter (mm)	190
Rotor thickness (mm)	20

Table (2) shows the meanings of some symbols in the potential and kinetical energy expressions.

Table 2. Symbols in the potential and kinetical energy expressions.

Symbol	Description
L	Length slender axis
ρ	Metal density
J	Inertial polar moment of slender axis cross section
J_1	Inertial moment of external rotor
J_M	Inertial moment of internal rotor
J_3	Inertial moment of rotor coupled to the motor output
n_M	Motor reduction
L_{ind}	Motor inductance
C_M	Motor internal damping
k_E	Velocity constant of the motor
k_T	Torque constant of the motor
$\bar{c}$	Motor current
G	Shear modulus of the slender axis
N_0	Average frictional normal force
R_s	Normal force application radius

Equations of motion are obtained using dimensionless parameters for simplicity. Table (3) lists the dimensionless parameters used to describe the motion.

Equations (2) and (3) present potential and generalized kinetical energy expressions as functions of dimensionless parameters. Functions $\bar{\theta}_j(x^*),\ j=1,2,\ldots,N,$ are the eigenfunctions for torsional system, analytically calculated, and $x^*=\dfrac{x}{L}$. L is the axis length.

$$U^* = \frac{L}{GJ}U = \frac{1}{2}\int_0^1 \left(\frac{\partial\theta}{\partial x^*}\right)^2 dx^* \tag{2}$$

$$T_c^* = \frac{L}{GJ}T_c = \frac{1}{2}\int_0^1 \left(\frac{\partial\theta}{\partial t^*}\right)^2 dx^* + \frac{1}{2}\gamma_1\left(\frac{\partial\theta}{\partial t^*}\bigg|_{x^*=1}\right)^2 + \frac{1}{2}\gamma_3\left(\frac{\partial\theta}{\partial t^*}\bigg|_{x^*=0}\right)^2 + \frac{L}{GJ}\frac{1}{2}L_{ind}\left(\frac{2\pi k_E}{R_A}\right)^2 \bar{c}^{*2} \tag{3}$$

Table 3. Dimensionless parameters in potential and kinetical energy expressions.

Parameter	Symbol	Dimensionless parameter	Scale constants
Position along the axis	x	$x^* = \frac{x}{L},\ 0 \le x^* \le 1$	L
Time	t	$t^* = \frac{t}{T_a}$	$T_a = \frac{L}{c};\ c = \sqrt{\frac{G}{\rho}}$
Motor input voltage	v	$v^* = \frac{v}{V_c}$	$V_c = 2\pi k_E$
Electrical current	$\bar{c}$	$\bar{c}^* = \frac{\bar{c}}{I_c}$	$I_c = \frac{V_c}{R_A};\ R_A$ is the electrical resistance
Electrical charge	q	$q^* = \frac{q}{Q_c}$	$Q_c = I_c T_a$
Inertial moment of external rotor	J_1	$\gamma_1 = \frac{J_1}{\rho JL}$	ρJL
Total inertial moment in $x = 0$	$\bar{J}_3 = n_M^2 J_M + J_3$	$\gamma_3 = \frac{n_M^2 J_M + J_3}{\rho JL}$	ρJL
Kinetical energy	T_c	$T_c^* = \frac{L}{GJ}T_c$	$\frac{GJ}{L}$
Potential energy	U	$U^* = \frac{L}{GJ}U$	$\frac{GJ}{L}$

Generalized forces is expressed as dimensionless formulation, with $\omega(x^*,t^*) = \frac{\partial\theta}{\partial t}(x^*,t^*) = \frac{\partial\theta}{T_a\partial t^*}(x^*,t^*)$ and time scale T_a, according Eq. (4), (5) and (6).

$$\eta_j{}^*(x^*=0,t^*) = \frac{L}{GJ}\eta_j(x^*=0,t^*) = \frac{L}{GJ}\left(n_M T_M - n_M^2 C_M \omega(x^*=0,t^*)\right)\bar{\theta}_j(x^*=0) \tag{4}$$

$$\eta_{s_j}{}^*(x^*=1,t^*) = \frac{L}{GJ}\eta_{s_j}(x^*=1,t^*) = \frac{L}{GJ}\left(\mu_0 N r \Phi\left(\frac{\omega(x^*=0,t^*)}{\omega_0}\right)\right)\bar{\theta}_j(x^*=1) \tag{5}$$

$$\eta^*{}_{D_j}(t^*) = \frac{L}{GJ}\eta_{D_j}(t^*) = \frac{L}{GJ}\int_0^1 D(x^*)\frac{\partial\theta}{\partial t}(x^*,t^*)\bar{\theta}_j(x^*)dx^* \tag{6}$$

An approach is made, as usual, for variable separation, that is expanding for modes and time functions, as shown in Eq. (7).

$$\theta(x^*,t^*) = \sum_{j=1}^{N}\xi_j(t^*)\bar{\theta}_j(x^*) \tag{7}$$

As previously stated, eigenfunctions and natural frequencies are analytically calculated. They are obtained from torsional wave equation and boundary conditions for the system illustrated in Fig. 2, according Eq. (8) and (9), already in dimensionless form.

$$\frac{\partial^2\theta}{\partial t^{*2}} = \frac{\partial^2\theta}{\partial x^{*2}} \tag{8}$$

$$\left.\frac{\partial\theta}{\partial x^*}\right|_{x^*=0} = \gamma_3 \left.\frac{\partial^2\theta}{\partial t^{*2}}\right|_{x^*=0}$$
$$\left.\frac{\partial\theta}{\partial x^*}\right|_{x^*=1} = -\gamma_1 \left.\frac{\partial^2\theta}{\partial t^{*2}}\right|_{x^*=1} \tag{9}$$

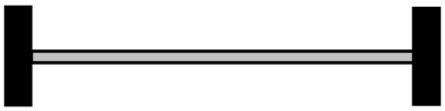

Figure 2. Torsional system. From left to right, rotor with inertial moment $\bar{J}_3 = n_M^2 J_M + J_3$, slender axis, and rotor with inertial moment J_1.

Analytical solutions for these equations include one rigid body frequency, $\lambda_1 = 0$, and an enumerable series of vibration frequencies $\lambda_2, \lambda_3, \lambda_4, \ldots$, solutions of Eq. (10), and eigenfunctions described in Eq. (11).

$$\left(\frac{1}{\gamma_1} - \lambda^2\gamma_3\right)\mathrm{sen}(\lambda) + \left(\frac{\gamma_3}{\gamma_1} + 1\right)\lambda\cos(\lambda) = 0 \tag{10}$$

$$\varphi_1(x^*) = 1$$
$$\varphi_j(x^*) = \cos(\lambda_j x^*) - \lambda_j\gamma_3\,\mathrm{sen}(\lambda_j x^*),\ j = 2, 3, 4, \ldots \tag{11}$$

Table (4) lists the first five analytical frequencies of the torsional system.

Table 4. Analytical natural frequencies of the torsional system.

i	λ_i	$\omega_i = \frac{\lambda_i}{T_a}(\mathrm{rad/s})$	$f_i = \frac{\omega_i}{2\pi}(\mathrm{Hz})$
1	0	0	0
2	0,0198	26,0	4,1
3	3,1417	4099,0	652,4
4	6,2832	8198,0	1304,7
5	9,4248	12.296,0	1957,0

Normalized eigenfunctions $\bar{\theta}_j(x^*),\ j = 1, 2, 3, 4, \ldots$ is defined as in Eq. (12):

$$\bar{\theta}_j(x^*) = \frac{\varphi_j(x^*)}{\|\varphi_j\|},\ j = 1, 2, 3, 4, \ldots \tag{12}$$

The norm is defined as in Eq. (13) and (14). The operator $M(\varphi_j, \varphi_i)$ is obtained from inertial matrix of the system dynamic weak formulation.

$$\|\varphi_j\| = \sqrt{\langle\varphi_j, \varphi_j\rangle} \tag{13}$$

$$\left\langle \varphi_j, \varphi_j \right\rangle = M\left(\varphi_j, \varphi_i\right) = \int_0^1 \varphi_j(x)\varphi_i(x)dx + \gamma_1\varphi_j(1)\varphi_i(1) + \gamma_3\varphi_j(0)\varphi_i(0) \tag{14}$$

Considering $\omega_j{}^* = \dot{\xi}_j{}^*,\ j = 1, 2, \ldots, N,$ the final dynamic equations for the electromechanical system are achieved, as Eq. (15). The parameters α, β and σ are dimensionless constants; z is the state variable vector of the system; and $F = F\left(\theta, \dot{\theta}\right)$ is defined in Eq. (1).

$$\dot{Z} = AZ - \tilde{F}(Z) + Bv^* \tag{15}$$

where:

$$Z = \left[\xi_1 \ \cdots \ \xi_N \ \ \omega_1{}^* \ \cdots \ \omega_N{}^* \ \ \bar{c}^*\right]^T,$$

$$B = \left[0 \ \cdots \ 0 \ \ 0 \ \cdots \ 0 \ \ \sigma\right]^T,$$

$$A = \begin{bmatrix} 0 & \cdots & 0 & 1 & \cdots & 0 & 0 \\ \vdots & \ddots & \vdots & \vdots & \ddots & \vdots & \vdots \\ 0 & \cdots & 0 & 0 & \cdots & 1 & 0 \\ -\lambda_1^2 & \cdots & 0 & -d_{11} & \cdots & -d_{1N} & n_M\beta\bar{\theta}_1(0) \\ \vdots & \ddots & \vdots & \vdots & \ddots & \vdots & \vdots \\ 0 & \cdots & -\lambda_N^2 & -d_{N1} & \cdots & -d_{NN} & n_M\beta\bar{\theta}_N(0) \\ 0 & \cdots & 0 & -n_M\alpha\bar{\theta}_1(0) & \cdots & -n_M\alpha\bar{\theta}_N(0) & -\sigma \end{bmatrix},$$

$$\tilde{F}(Z) = \frac{L}{GJ}F\left(\theta\left(x^* = 1, t^*\right), \dot{\theta}\left(x^* = 1, t^*\right)\right)\left[0 \ \cdots \ 0 \ \ \bar{\theta}_1(1) \ \cdots \ \bar{\theta}_N(1) \ \ 0\right]^T.$$

2.2 Normal form of dynamic model

In order to implement sliding control, it is necessary to start from the dynamical equation in normal form. The system output, which is also the parameter to be controlled, is the angular velocity of external rotor, as in Eq. (16).

$$y = \frac{\partial\theta}{\partial t^*}\left(x^* = 1, t^*\right) = \sum_{j=1}^{N}\omega_j{}^*(t^*)\bar{\theta}_j(1) = \tilde{\omega}^*(t^*)^T\left[\bar{\theta}(1)\right] \tag{16}$$

where $\tilde{\omega}^*(t^*) = \left[\omega_1{}^* \ \ \omega_2{}^* \ \cdots \ \omega_N{}^*\right]^T$ and $\left[\bar{\theta}(x^*)\right] = \left[\bar{\theta}_1(x^*) \ \ \bar{\theta}_2(x^*) \ \cdots \ \bar{\theta}_N(x^*)\right]^T$.

Calculating the time derivatives $\dot{y}$ and $\ddot{y}$:

$$\begin{aligned} &\dot{y} = \left(-\tilde{\xi}^T K^T - \tilde{\omega}^T D^T - F(Z)\left[\bar{\theta}(1)\right]^T + n_M\beta\left[\bar{\theta}(0)\right]^T\bar{c}\right)\left[\bar{\theta}(1)\right] \Rightarrow \\ &\Rightarrow \dot{y} = -\tilde{\xi}^T K^T\left[\bar{\theta}(1)\right] - \tilde{\omega}^T D^T\left[\bar{\theta}(1)\right] - F(Z)\sigma_{11} + n_M\beta\sigma_{01}\bar{c} \end{aligned} \tag{17}$$

$$\ddot{y} = \alpha_l Z + \alpha_{nl_2}F(Z) - \alpha_{nl}\nabla F(Z)\left(AZ - \tilde{F}(Z)\right) + bv^* \tag{18}$$

with the following terms in Eq. (17) and Eq. (18):

$$\sigma_{01} = \left[\bar{\theta}(0)\right]^T\left[\bar{\theta}(1)\right]$$

$$\sigma_{11} = \left[\bar{\theta}(1)\right]^T\left[\bar{\theta}(1)\right]$$

$$K = \begin{bmatrix} \lambda_1^2 & \cdots & 0 \\ \vdots & \ddots & \vdots \\ 0 & \cdots & \lambda_N^2 \end{bmatrix}$$

$$D = \begin{bmatrix} d_{11} & \cdots & d_{1N} \\ \vdots & \ddots & \vdots \\ d_{N1} & \cdots & d_{NN} \end{bmatrix} = \begin{bmatrix} \bar{d}_1(\lambda_1) & \bar{d}_2(\lambda_2) & \cdots & \bar{d}_N(\lambda_N) \end{bmatrix}$$

$$\alpha_l = \begin{bmatrix} \alpha_{l\xi} & \alpha_{l\omega} & \alpha_{l\bar{c}} \end{bmatrix}$$

$$\alpha_{l\xi} = \left[\bar{\theta}(1)\right]^T DK$$

$$\alpha_{l\omega} = -\left[\bar{\theta}(1)\right]^T K + \left[\bar{\theta}(1)\right]^T D^2 - n_M^2 \alpha\beta\left[\bar{\theta}(0)\right]^T \sigma_{01}$$

$$\alpha_{l\bar{c}} = -n_M\beta\left[\bar{\theta}(1)\right]^T D\left[\bar{\theta}(0)\right] - n_M\beta\sigma\sigma_{01}$$

$$\alpha_{nl} = \left[\bar{\theta}(1)\right]^T \left[\bar{\theta}(1)\right] = \sigma_{11}$$

$$\alpha_{nl_2} = \left[\bar{\theta}(1)\right]^T D\left[\bar{\theta}(1)\right]$$

$$b = n_M\beta\sigma\sigma_{01}$$

In fact, relative degree of the system is $r = 2,$ and it can be rewritten in terms of normal variables, as in Eq. (19).

$$\ddot{y} = a(X) + bv^* \tag{19}$$

where $a(X) = \alpha_l Z + \alpha_{nl_2} F(Z) - \alpha_{nl} \nabla F(Z)\left(AZ - \tilde{F}(Z)\right)$ and $X = \begin{bmatrix} \tilde{\mu} \\ \tilde{\psi} \end{bmatrix} = \begin{bmatrix} \mu_1 & \mu_2 & \psi_1 & \cdots & \psi_{2N-1} \end{bmatrix}^T$.

Vectors X and Z are related by a diffeomorphism Φ_{dif} as in Eq. (20).

$$X = \Phi_{dif}(Z) = \sigma_{xl} Z - \sigma_{xnl} F(Z) \tag{20}$$

where

$$\sigma_{xl} = \begin{bmatrix} 0_{1\times N-1} & & \left[\bar{\theta}(1)\right]^T & & 0 \\ -\left[\bar{\theta}(1)\right]^T K & & -\left[\bar{\theta}(1)\right]^T D & & n_M\beta\sigma_{01} \\ I_{N-1} & 0_{N-1\times 1} & 0_{N-1} & 0_{N-1\times 1} & 0_{N-1\times 1} \\ 0_{N-1} & 0_{N-1\times 1} & I_{N-1} & 0_{N-1\times 1} & 0_{N-1\times 1} \\ 0_{1\times N-1} & 1 & 0_{1\times N-1} & 0 & 0 \end{bmatrix},$$

and

$$\sigma_{xnl} = \begin{bmatrix} 0 & \sigma_{11} & 0 & \cdots & 0 \end{bmatrix}^T.$$

The variables ψ_j are chosen so that Φ_{dif} is a diffeomorphism and $\nabla\psi_j B = \dfrac{\partial\psi_j}{\partial z_{2N+1}}\sigma = 0 \Rightarrow \dfrac{\partial\psi_j}{\partial z_{2N+1}} = 0$ is satisfied for $j = 1, 2, \ldots, 2N-1$ (Slotine, 1991). Then, internal dynamics of the system is obtained so that:

$$\dot{\psi}_j = \nabla\psi_j \dot{Z} = \nabla\psi_j \left[AZ - \tilde{F}(Z) + Bv^* \right] = \nabla\psi_j \left[AZ - \tilde{F}(Z) \right] + \nabla\psi_j B v^* \Rightarrow \dot{\psi}_j = \nabla\psi_j \left[AZ - \tilde{F}(Z) \right] \tag{21}$$

As a result, Eq. (19) and Eq. (21) are rewritten in a more explicit form, as in Eq. (22).

$$\begin{bmatrix} \dot{\mu}_1 \\ \dot{\mu}_2 \\ \dot{\psi}_1 \\ \dot{\psi}_2 \\ \vdots \\ \dot{\psi}_{N-1} \\ \dot{\psi}_N \\ \vdots \\ \dot{\psi}_{2N-2} \\ \dot{\psi}_{2N-1} \end{bmatrix} = \begin{bmatrix} \mu_2 \\ a(X) + bv \\ \psi_N \\ \psi_{N+1} \\ \vdots \\ \psi_{2N-2} \\ -\lambda_1^2 z_1 - \sum_{j=1}^{N} d_{1j} z_{N+j} - F(Z)\bar{\theta}_1(1) \\ \vdots \\ -\lambda_1^2 z_1 - \sum_{j=1}^{N} d_{1j} z_{N+j} - F(Z)\bar{\theta}_{N-1}(1) \\ z_{2N} \end{bmatrix} \tag{22}$$

3. CONTROL LAW

For purposes of simulation, it is assumed an uncertainty in friction normal force so that:

$$N_0 \sim \hat{N}_0 \pm \Delta N \tag{23}$$

N_0 is the real value of the normal force, and $\hat{N}_0$ is the estimated one.

3.1 Desired trajectory

The desired trajectory for system is to maintain the external rotor at a predefined constant angular velocity $\omega_{ref}\ (rad/s)$, which means that, in terms of state variable, $\xi_j = 0$ and $\omega_j{}^* = 0$ for $j = 2, \ldots, N$, and:

$$z_{N+1_d} = \omega_1{}^*(t^*) = \frac{T_0 \omega_{ref}}{\bar{\theta}_1(1)} \tag{24}$$

$$z_{1_d} = \xi_1(t^*) = \frac{T_0 \omega_{ref}}{\bar{\theta}_1(1)} t^* \tag{25}$$

To calculate desired value for $z_{2N+1} = \bar{c}^*(t^*)$ in steady state, first it is necessary to consider $\ddot{y} = 0$ in Eq. (19), so that:

$$v^* = -\frac{1}{b} a(X_d) \tag{26}$$

On the other hand, motor electrical circuit is modeled as Eq. (27).

$$\dot{\bar{c}}^* + n_M \alpha \sum_{j=1}^{N} \omega_j{}^*(t^*)\bar{\theta}_j(1) + \sigma \bar{c}^* = \sigma v^* \tag{27}$$

Considering steady state of the system in the desired trajectory, $\dot{\bar{c}}^* = 0$. In fact that, from Eq. (26) and Eq. (27) we conclude that:

$$n_M\alpha\left(T_0\omega_{ref}\right)+\sigma z_{2N+1_d}+\sigma\frac{1}{b}\hat{a}\left(\Phi_{dif}\left(Z_d\right)\right)=0 \tag{28}$$

The desired state in steady regime $z_d=\left[z_{1_d}\ \ 0\ \cdots\ 0\ \ z_{N+1_d}\ \ 0\ \cdots\ 0\ \ z_{2N+1_d}\right]^T$ contains the parameter z_{2N+1_d}, that is calculate from Eq. (28) from Newton-Raphson method.

3.2 Control law by sliding modes

Let $S(t^*)$ be a time-varying surface in R^r space, defined as Eq. (29), considering $\tilde{y}=y-y_d$.

$$s(X;t^*)=\left(\frac{d}{dt^*}+\lambda\right)^{r-1}\tilde{y}=0 \tag{29}$$

System has relative degree $r=2$, and from Eq. (29), we conclude that:

$$s=\dot{\tilde{y}}^*+\lambda\tilde{y}=\dot{y}^*-\dot{y}_d^*+\lambda\left(y-y_d\right) \tag{30}$$

$$\dot{s}^*=\ddot{\tilde{y}}^*+\lambda\dot{\tilde{y}}^*=\ddot{y}^*-\ddot{y}_d^*+\lambda\left(\dot{y}^*-\dot{y}_d^*\right) \tag{31}$$

Substituting Eq. (19) into Eq. (31), result in Eq. (32):

$$\dot{s}^*=a\left(\Phi_{dif}\left(Z\right)\right)+bv^*-\ddot{y}_d^*+\lambda\dot{\tilde{y}}^* \tag{32}$$

Let $\hat{a}(X)$ be an approximated function of $a(X)$ for average value $\hat{N}_0$ of friction normal force:

$$\hat{a}(Z)=\alpha_l Z-\alpha_{nl}\mu_0\hat{\tau}_{N_0}\nabla\bar{\Phi}(Z)AZ+\alpha_{nl}\mu_0^2\hat{\tau}_{N_0}^2\nabla\Phi(Z)\tilde{\Phi}(Z) \tag{33}$$

with the terms: $\hat{\tau}_{N_0}=\frac{L}{GJ}\hat{N}_0R_s$, $\bar{\Phi}(Z)=\Phi\left(\frac{\dot{\theta}}{\omega_0}\right)\left(1+\beta_N sen(\theta)\right)$ and $\tilde{\Phi}(Z)=\bar{\Phi}(Z)\left[0\ \ \cdots\ \ 0\ \ \bar{\theta}_1(1)\ \ \cdots\ \ \bar{\theta}_N(1)\ \ 0\right]^T$.

The variation $\Delta a(Z)=\hat{a}-a$ is estimated as in Eq. (34):

$$\Delta a(Z)\cong\frac{\partial\hat{a}}{\partial\tau_{N_0}}\Delta\tau_{N_0}=\left[\alpha_{nl}\mu_0\Phi(Z)-\alpha_{nl}\mu_0\nabla\Phi(Z)AZ+2\alpha_{nl}\mu_0^2\tau_{N_0}\nabla\Phi(Z)\tilde{\Phi}(Z)\right]\Delta\tau_{N_0} \tag{34}$$

Let $\bar{F}(Z)$ be so that:

$$\bar{F}(Z)=\left|\Delta\tau_{N_0}\right|\left|\alpha_{nl}\mu_0\Phi(Z)-\alpha_{nl}\mu_0\nabla\Phi(Z)AZ+2\alpha_{nl}\mu_0^2\tau_{N_0}\nabla\Phi(Z)\tilde{\Phi}(Z)\right|\geq\left|\Delta a(Z)\right|=\left|\hat{a}-a\right|$$

The control law is defined considering $\dot{s}^*=0$ in Eq. (32). Then:

$$\hat{v}(Z)=\frac{1}{b}\left(-\hat{a}(Z)+\ddot{y}_d-\lambda\dot{\tilde{y}}\right) \tag{35}$$

Assuming a variable saturation band Φ_{bd}, the sliding condition to be satisfied by control law is:

$$\frac{1}{2}\frac{ds^2}{dt}\leq\left(\dot{\Phi}_{bd}-\eta\right)|s|,\quad |s|>\Phi_{bd} \tag{36}$$

Thus, the final control law is:

$$v(Z) = \hat{v}(Z) - \frac{\bar{k}(Z)}{b}\,\mathrm{sat}\left(\frac{s}{\Phi_{bd}}\right) \tag{37}$$

with the terms: $\bar{k}(Z) = k(Z) - \dot{\Phi}_{bd}$ and $k(Z) = \bar{F}(Z) + \eta$.

According Slotine (1991), for $|s| < \Phi_{bd}$, it is possible to demonstrate that:

$$\dot{s} = -\bar{k}(Z)\frac{s}{\Phi_{bd}} - \Delta a(Z) \cong -\bar{k}(Z_d)\frac{s}{\Phi_{bd}} - \Delta a(Z_d) + O(\varepsilon) \tag{38}$$

Equation (38) model a low pass filter with input $-\Delta a(Z_d) + O(\varepsilon)$. In order to filter frequencies above λ, it is necessary that:

$$\frac{\bar{k}(Z_d)}{\Phi_{bd}} = \lambda \tag{39}$$

However, considering $\bar{k}(Z_d) = k(Z_d) - \dot{\Phi}_{bd}$, and substituting this condition in Eq. (39), we conclude:

$$\begin{cases} \dot{\Phi}_{bd} + \lambda\Phi_{bd} = k(Z_d) \\ \Phi_{bd}(0) = \dfrac{k(Z_d(0))}{\lambda} \end{cases} \tag{40}$$

The condition $\Phi_{bd}(0) = k(Z_d(0))\lambda^{-1}$ guarantees $\dot{\Phi}_{bd}(0) = 0$.

4. SIMULATIONS

Equations (15), (37) and (40) are integrated by Runge-Kutta method, order 4, with constant step size $\Delta t^* = 10^{-5}$. Input parameters are:

1. $N = 3$, number of system modes;
2. $\eta^* = 1.48 \times 10^{-6}$, sliding mode parameter. The reach time is so that $t_{reach}{}^* \le \dfrac{|s(t^* = 0)|}{\eta^*}$.

   Considering the project parameter $t_{reach} = 5.0\,s$, so:

   $$\eta^* \le \frac{|s(t^* = 0)|}{t_{reach}{}^*} \cong \frac{\lambda y_d T_a}{t_{reach}} = \frac{2 \times 6.24 \times T_a^2}{5.0} = \frac{2 \times 6.24 \times \left(7.8856 \times 10^{-4}\right)^2}{5.0} \cong 1.55 \times 10^{-6}$$

3. $\lambda = 2 < \dfrac{1}{3}\upsilon_{N+1}$. $\upsilon_{N+1} = \upsilon_4 = 6{,}28$ is the minor non modeled dimensionless frequency of the system (Slotine, 1991).
4. $N_0 = 1N$, friction normal force, and $\beta_N = 0.1$, normal force intensity oscillation coefficient, as in Eq. (01).
5. $\omega_{ref} = 60rpm$, desired angular velocity.

Figure 3 shows the external rotor reaching the desired speed about $5.0\,s$ after the rest initial state.

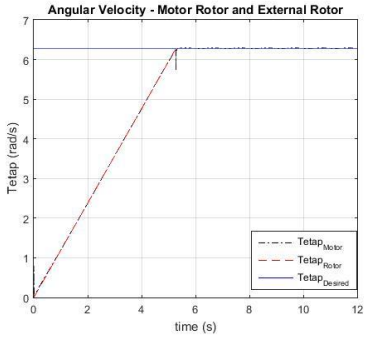

Figure 3. Angular velocities of the rotors.

The external rotor starts from the rest state with a relative delay, respect to the motor rotor. At the beginning, the motor rotor reaches a velocity peak of $0.8\,rad/s$, as shown in fig. 4a.

On the other hand, fig. 4b illustrates an abrupt reduction of the motor rotor angular velocity in approximately $0.6\,rad/s$, some milliseconds before external rotor reaches the desired angular velocity, which ensures external rotor deceleration.

Figure 5 shows the moment when the sliding variable s reaches the boundary layer, $t_{reach} \cong 5.3\,s$, which is the same instant when the external rotor reaches the desired angular velocity. The simulation value of t_{reach} is approximately equal to the nominal one.

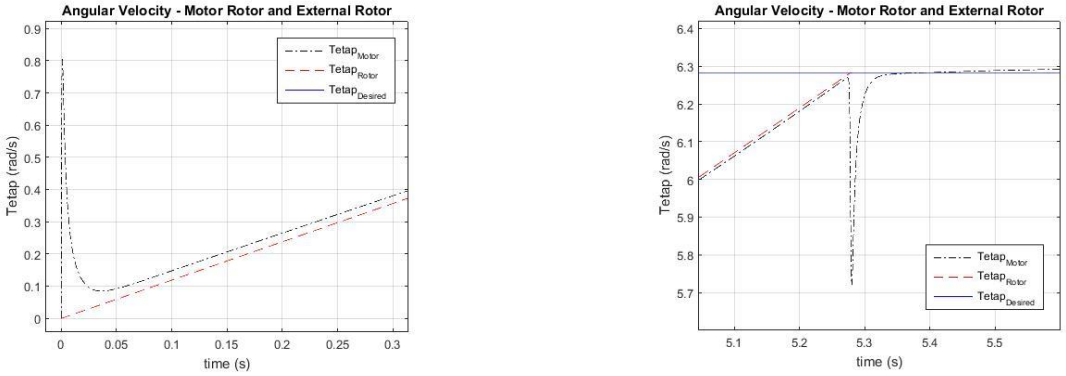

(a) (b)

Figure 4. Angular velocities of the rotors (zoom).

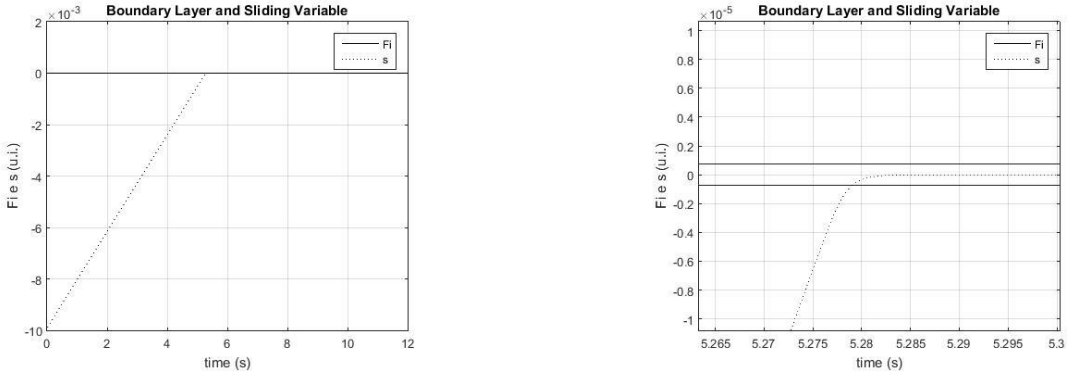

Figure 5. Boundary Layer and Sliding Variable over time.

A common problem in implementing the sliding mode technique is the high frequency switching at the actuator input. This phenomenon is known in the literature as *chattering*. Therefore, the sliding mode technique is implemented with a saturation band at this work, as in Eq. (36). This allows smoothing the input voltage on the motor.

Figure 6 illustrates the input voltage over time. As we can see, *chattering* phenomenon does not occur.

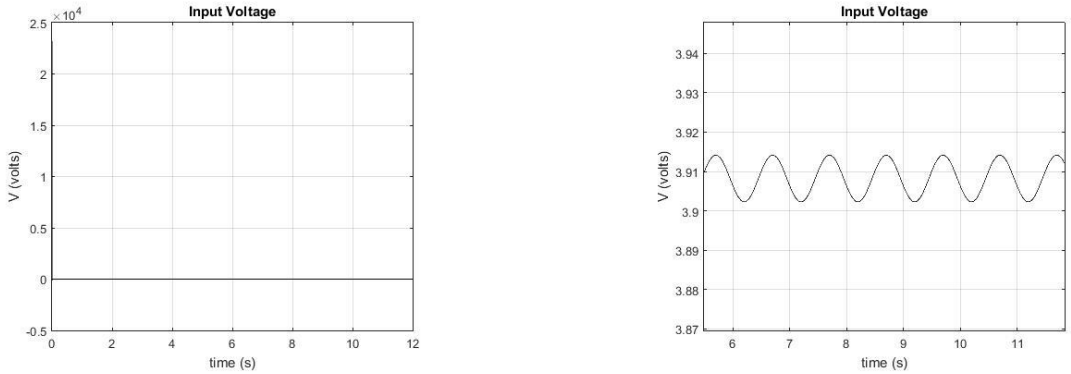

Figure 6. Input voltage over time. No chattering.

On the other hand, Figure 7 shows oscillations in the steady state, both in the angular velocity of the motor rotor and in the input voltage. This occurs to ensure a constant angular velocity of the external rotor, in spite of the frictional normal force oscillation.

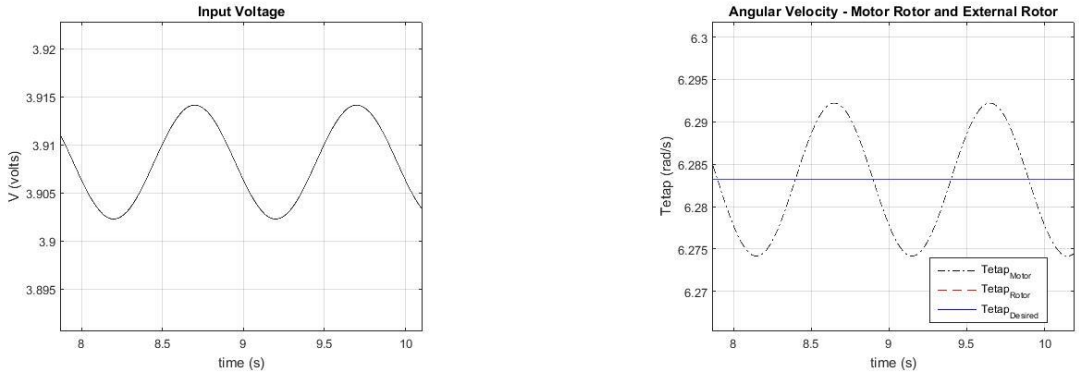

(a) (b)

Figure 7. Oscillations (a) in input voltage curve, (b) in rotors angular velocity.

Other important facts in fig. 8 are the peaks of electrical current and input voltage. They indicate that the desired trajectory should possibly be smoother by taking the system out of rest.

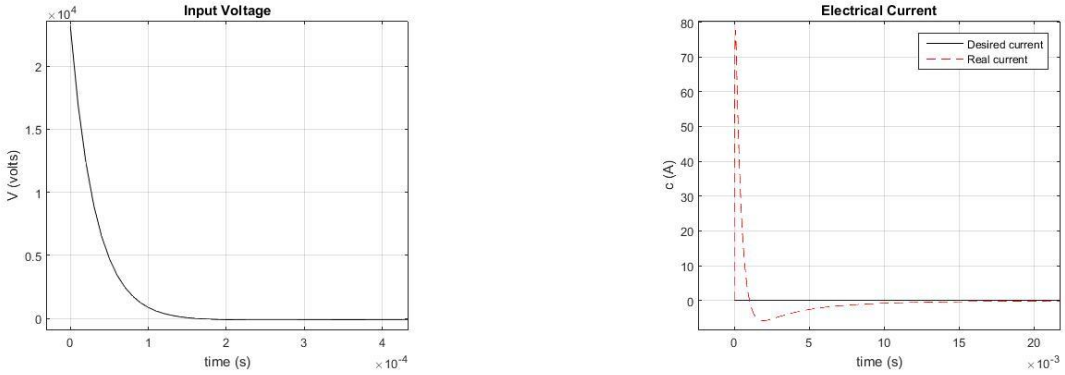

(a) (b)

Figure 8. Peaks (a) in input voltage curve, and (b) in electrical current curve.

Finally, Fig. 9 shows the system trajectory by means of the observed variable phase diagram. The system remains within the saturation band after reaching it. The system then assumes the desired angular velocity condition of $60 rpm$ ($6.28 rad/s$), and null angular acceleration.

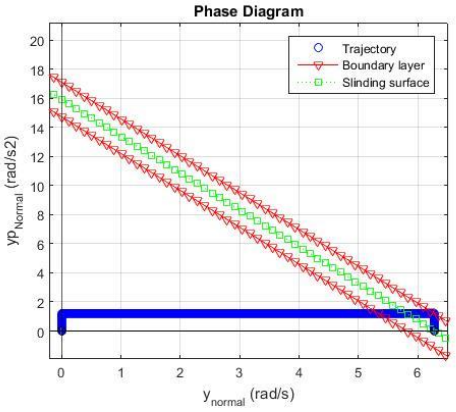

Figure 9. Phase Diagram

5. CONCLUSIONS

This work aims to present a robust control strategy to stabilize the angular velocity of a flexible and slender rotary system, subject to dry friction.

The adopted technique presents good results. The desired state for the system is reached after a small time interval. The use of a variable saturation band has avoided the chattering problem in the input voltage, which was evident by the soft curve presented by the input voltage in time.

On the other hand, the high peaks observed in the voltage and current graphs at the time of starting the system were an inconvenience, and indicated the degree of dependence that exists between the control performance and the appropriate adjustment of the parameters. This result suggests a redefinition of the desired trajectory for the system, in order to smooth the transition from rest to the desired final state.

6. REFERENCES

Abdulgalil, F. and Siguerdidjane, H., 2005. "PID Based on Sliding Mode Control for Rotary Drilling System". In *EUROCON 2005*. Belgrade, Servia e Montenegro.

Andrade, B.C.C., 2013. *Numerical and experimental analysis of nolinear torsional dynamics of a drilling system.* Masters dissertation, Pontifícia Universidade Católica do Rio de Janeiro, Brazil.

Christoforou, A.P. and Yigit, A.S. Fully coupled vibrations of actively controlled drillstrings. "Journal of Sound and Vibration". 2005. Vol. 267, p.1029-1045.

López, E.M.N. and Castro, E.L., 2009. Non-desired transitions and sliding-mode control of a multi-DOF mehcanical system with stick-slip oscillations. Chaos, Solitons and Fractals. 2009. Vol. 41, p.2035-2044.

López, E.M.N. and Cortés, D., 2007. "Sliding-mode control of a multi-DOF oilwell drillstring with stick-slip oscillations". In *Proceedings of the American Control Conference*. New York City, USA.

Slotine, J.E. and Li, W., 1991. *Applied nonlinear control*. Prentice-hall, New York.

Zhang, Q., He, Y., Li, L. and Nurzat, N., 2010. "Sliding Mode Control of Rotary Drilling System with Stick Slip Oscillation". In *2nd International Workshop on Intelligent Systems and Applications – ISA2010*. Wuhan, China.

7. RESPONSIBILITY NOTICE

The authors are the only responsible for the printed material included in this paper.